

Self-confinement of finite dust clusters in isotropic plasmas

G. V. Miloshevsky* and A. Hassanein

Center for Materials under Extreme Environment, School of Nuclear Engineering, Purdue University, 400 Central Drive, West Lafayette, Indiana 47907-2017, USA

(Received 29 August 2011; revised manuscript received 23 February 2012; published 15 May 2012)

Finite two-dimensional dust clusters are systems of a small number of charged grains. The self-confinement of dust clusters in isotropic plasmas is studied using the particle-in-cell method. The energetically favorable configurations of grains in plasma are found that are due to the kinetic effects of plasma ions and electrons. The self-confinement phenomenon is attributed to the change in the plasma composition within a dust cluster resulting in grain attraction mediated by plasma ions. This is a self-consistent state of a dust cluster in which grain's repulsion is compensated by the reduced charge and floating potential on grains, overlapped ion clouds, and depleted electrons within a cluster. The common potential well is formed trapping dust clusters in the confined state. These results provide both valuable insights and a different perspective to the classical view on the formation of boundary-free dust clusters in isotropic plasmas.

DOI: [10.1103/PhysRevE.85.056405](https://doi.org/10.1103/PhysRevE.85.056405)

PACS number(s): 52.27.Lw, 52.65.Rr

I. INTRODUCTION

Controlled manipulation, assembly, and disassembly of finite clusters of particles are of great importance in physics and chemistry [1]. Different types of atomic and molecular clusters were observed on the atomistic scale [2]. Their configurations and dynamical properties are strongly influenced by the number of particles in a cluster. The understanding of the physics and their behavior is important for the development of nanomaterials, microstructures, and microdevices [1]. The two-dimensional (2D) finite dust clusters in complex plasmas are of fundamental interest since dust grains can be easily visualized and studied at the kinetic level. Therefore, the theoretical and experimental studies of finite 2D dust clusters composed of just a few grains are important for the understanding of grain coupling, arrangements, closed shell configurations, instabilities, and structural transitions. Small 2D clusters of dust grains were investigated in several experiments utilizing an external confining potential [3–5]. It was found that the grains are arranged in stable ringlike concentric shells. The existence of boundary-free (unconfined) clusters was also predicted [6]. The formation of dusty plasma molecules from two dust grains surrounded by Debye plasma spheres (dressed grains) has been predicted theoretically [7,8]. The energy of interaction between grains was described by four terms corresponding to that between two grains, two Debye spheres, and grain-Debye sphere interactions (two cross terms describing shielding effects). It was demonstrated that the potential energy as a function of intergrain separation is reminiscent of a form of van der Waals curve with repulsion, equilibrium, and attraction regions [7,8]. The dust self-organization into a cluster in the absence of any external confining potential was predicted using molecular dynamics (MD) simulations [9]. It was shown theoretically that a stable 2D grain cluster can exist in plasmas without external confinement [10]. It is very difficult to create the boundary-free dust clusters in laboratory experiments. The effects of walls, gravity, external electric or magnetic fields, and ion drag forces

have to be eliminated. This can be achieved in experiments performed in space. An attraction of dust grains in the bulk region of the plasma with isotropic plasma conditions was indeed observed in a recent experiment under microgravity conditions [11]. A boundary-free dust cluster was formed from a large central grain and a number of peripheral small grains (six times smaller). The attraction between the like-charged grains was explained as due to the noncollective shadow force of plasma particles [6,9,10]. The idea is that the flux and momentum of plasma particles on grains forming a cluster is larger on the outer side than that on the inner side creating the pressure confining the dust grains in the bulk plasma.

A detailed quantitative-level modeling of complex plasma is highly challenging due to nonlinearity, large spatial and time-scale differences, and strong plasma-dust coupling. The MD method is a very useful tool [12]. However, the interaction potentials determined for a single grain cannot be used to describe the effects of collective charging and screening in a many-grain plasma system [13]. The explicit ions and electrons must be included. The plasma kinetics around one and two grains was studied using the fully kinetic MD model that treats explicitly electrons, ions, and dust charging [14,15]. However, this MD simulation was limited to $\sim 20\,000$ plasma particles. The particle-in-cell (PIC) method provides a self-consistent, fully kinetic description of complex plasmas with the ability to treat plasma-grain interactions [16]. The number of physical assumption in PIC models is minimally reduced retaining the most relevant physics. The dust charging and screening, nonlinear, and collective effects are included self-consistently. Fully kinetic PIC studies up to now have basically only focused on one or two dust grains [17,18].

In this paper, we investigated the self-confinement of 2D finite clusters consisting of 2, 3, 7, and 19 insulating grains immersed in isotropic plasma using the self-consistent, fully kinetic PIC method. The distribution of plasma electrons and ions is modeled in the presence of preconfigured dust clusters with variable intergrain separations. Our focus is on the fundamental physical processes of plasma-grain as well as intergrain interactions. The PIC model does not involve any phenomenological adjustable parameters and assumptions about the form of interactions with attractive or repulsive

*gennady@purdue.edu

potentials. Therefore, the results shed light on many interesting aspects of plasma-grain interactions, mediation of intergrain attraction by plasma ions, distribution of electric potential, and distributions of electrons and ions within a dust cluster. The results are significant for understanding the fundamental phenomena of self-confinement of dust grains into a cluster in the absence of the external confining potential.

II. PIC MODEL

Many technical details implemented in our self-consistent, fully kinetic 2D PIC code are conventional to PIC plasma models described in classical textbooks [16,19]. Peculiar features of our PIC model are accurate resolution of (1) finite size of small dust grains and (2) trajectories of plasma macroparticles close to the dust grains with treatment of short-range forces using direct plasma particle-grain force calculations [20]. A number of reduced time steps are used for plasma macroparticles in the vicinity of dust grains to resolve their trajectories within the size of grains [21]. This implementation was needed to correctly determine the charge and floating potential on grains. The multifrontal massively parallel solver MUMPS [22] is used to solve the Poisson equation during each time step. It is an accurate direct method based on lower and upper matrix factorization. The MUMPS solver utilizes the MPI library for message passing and uses the BLAS, BLACS, and SCALAPACK libraries.

The setup of the system is as follows. The computational domain represents a 2D plane with X and Y lengths of 0.01 m in Cartesian coordinates (Fig. 1). A grid with spacing $h = 50 \mu\text{m}$ (200×200 cells) is used. On the domain's boundaries, the electric potential is assumed fixed corresponding to that of unperturbed bulk plasma, ~ 0 V. The electron number density

and temperature are $N_e = 10^{15} \text{ m}^{-3}$ and $T_e = 3 \text{ eV}$ resulting in an electron Debye length of $\lambda_{D_e} \approx 407.2 \mu\text{m}$. The number of electron Debye lengths per domain length is ~ 25 . The electron plasma frequency is $\omega_e \sim 1.8 \times 10^9 \text{ s}^{-1}$. The ion number density N_i is the same as that of electrons. The ion temperature is $T_i = 0.03 \text{ eV}$ yielding $T_i/T_e = 0.01$. The ratio of ion to electron mass was set to 200. The ion Debye length is $\lambda_{D_i} \approx 40.7 \mu\text{m}$. The total Debye length is $\lambda_D \approx 40.5 \mu\text{m}$. For proper PIC simulations, the chosen grid step of $h = 50 \mu\text{m}$ satisfies the following condition $h < 3.4\lambda_D \sim 138 \mu\text{m}$ [19]. Thermal velocities of macroelectrons and macroions are $v_e \sim 7.3 \times 10^5 \text{ m/s}$ and $v_i \sim 5.1 \times 10^3 \text{ m/s}$, respectively. The time step is $\sim 10 \text{ fs}$; that is, $\sim 0.02/\omega_e$. The total number of simulation macroparticles (macroelectrons plus macroions) initially placed within the computational domain is $\sim 2 \times 10^6$. Each real plasma particle is represented by one macroparticle. The number of macroparticles per cell is ~ 50 . Plasma macroparticles are free to leave the computational domain through any boundary, and new plasma macroparticles can be injected from the boundaries of the computational domain. The plasma at the boundaries is modeled as unperturbed. The injecting boundaries maintain the flux of macroparticles with the Maxwellian velocity distributions. The modeled region effectively represents an infinite plasma system of large spatial extent. The dust grains with radius of $5 \mu\text{m}$ were initially preconfigured into symmetric dust clusters with a different number of grains. The separation distance between grains was scaled around the electron Debye length. Grains were treated as insulating infinite cylinders in 2D Cartesian coordinates. Because of the small grain size much smaller than Debye length, the charge distribution on the surface of the insulating dust grains due to the absorption of macroparticles was considered to be uniform. The simulations were run up to $\sim 5 \mu\text{s}$ (~ 100 ion plasma periods). On this ion time scale, the dust grains are immobile due to their large mass. Thus, the entropy contribution due to grains is not included. The Poisson equation is solved in the 2D Cartesian coordinates on the XY plane (Fig. 1). We follow the finite difference scheme described by Birdsall and Langdon in their classical book on PIC modeling [16], but we use the advanced parallel solver, MUMPS [22].

III. NUMERICAL RESULTS

For the analysis of the distribution of plasma electrons and ions, a region of the plasma covering the variable size of the dust cluster with 19 grains is illustrated in Fig. 2. The influence of grains on plasma structure is significant. It is seen that the plasma is strongly perturbed within the area of the dust cluster. The number of ions in the vicinity of a dust cluster is much greater than that in unperturbed plasma. The formation of these dense ion clouds can be attributed to the screening of highly negative charge on grains. The ions are collected around the grains, and the number of electrons is highly depleted within the cluster area. At separations $< \sim 400 \mu\text{m}$ [Figs. 2(a) and 2(b)], a uniform cloud of ions is formed covering the entire dust cluster. At large separations $> \sim 400 \mu\text{m}$ [Figs. 2(c) and 2(d)], there are isolated dense clouds of plasma ions surrounding the dust grains. The number of ions increases by ~ 8 – 10 times within the area of the dust cluster with scaling its size from $\sim 680 \mu\text{m}$ [Fig. 2(a)] to $\sim 2920 \mu\text{m}$ [Fig. 2(d)]. The dynamics

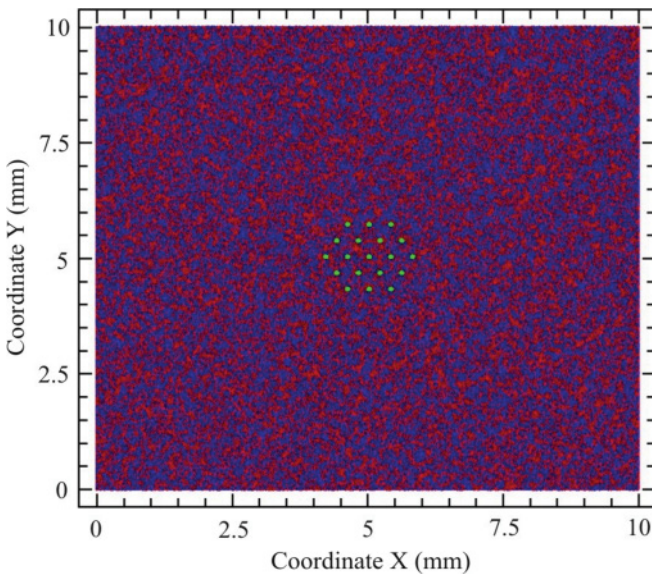


FIG. 1. (Color online) Representative sketch of the computational domain used in PIC simulations of dust clusters. There are $\sim 10^6$ electrons (blue (dark gray) points) and $\sim 10^6$ ions (red (light gray) points) resulting in a solid-colored computational domain. A dust cluster with 19 grains immersed in isotropic plasma is shown as green (white) spheres. For visibility, the size of grains is increased by 10 times.

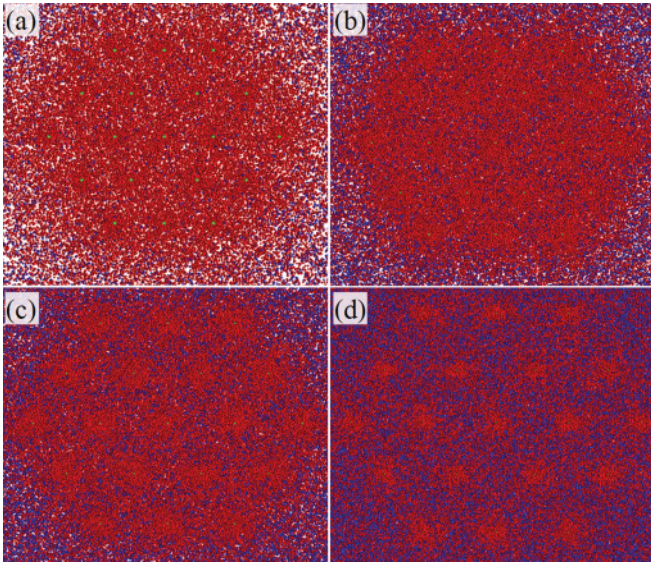


FIG. 2. (Color online) The distribution of plasma electrons (blue (dark gray) points) and ions (red (light gray) points) within the dust cluster consisting of 19 grains at time $\sim 5 \mu\text{s}$. Dust grains with radius of $5 \mu\text{m}$ are hardly visible as green (white) spheres in panel (a). The average distance between grains is (a) ~ 170.1 , (b) ~ 328.1 , (c) ~ 402.1 , and (d) $\sim 729.8 \mu\text{m}$.

of plasma ions and electrons within the scalable dust clusters consisting of 7 and 19 grains can be viewed in supplementary movies [23].

The profile of the electric potential across the dust cluster at $Y = 5 \text{ mm}$ is shown in Fig. 3 for various intergrain separations. At large separations between grains $\sim 730 \mu\text{m}$, the potential has five distinct wells with the central one disposed about $X = 5 \text{ mm}$. Even at these large separations, the potential barrier between the two adjacent wells is still a bit smaller compared to the bulk plasma potential. With decreasing the distance between grains, the multiple isolated potential wells merge into

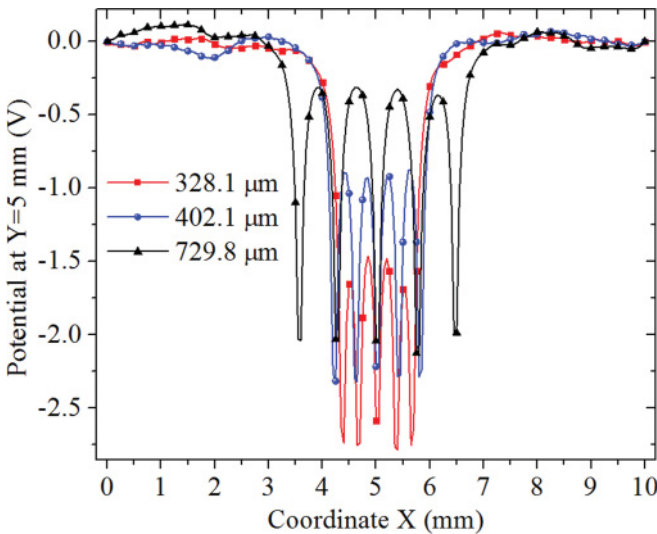


FIG. 3. (Color online) The cut-off potential on the grid at $Y = 5 \text{ mm}$ for the dust cluster with various separations between 19 grains at time $\sim 5 \mu\text{s}$.

a common potential well. At small separations $< \sim 400 \mu\text{m}$, the overall potential boundary around the dust cluster is formed. These potential transformations are determined by the charges on grains, the plasma composition, and the plasma charge density within a cluster (Fig. 2).

It is known that complex plasmas represent a thermodynamically open system [13]. The losses of electrons and ions on grains have to be compensated by external plasma and energy sources. Although the complex plasma is a non-Hamiltonian system, it was recently demonstrated for two dust grains in a plasma sheath that the Hamiltonian description can be used to provide valuable insights into the stability of dust clusters [24]. The plasma and energy supply is fast enough compensating the rate of plasma absorption on grains. The equilibrium charge on dust grains is maintained by these fluxes of electrons and ions that continuously exist after the stationary state is reached. The energy of the entire plasma-dust system can serve as an indicator for reaching the steady state. The time evolution of the total energy of the plasma-dust system [see Fig. 4(b)] demonstrates that cluster configurations with intergrain separations $\sim 328 \mu\text{m}$ are energetically more favorable compared to other configurations with smaller or larger intergrain separations [Fig. 4(a)]. During the first ion plasma period, the plasma-dust system undergoes a sharp transition. The changes of the total energy indicate charging of grains and the buildup of a sheath within a dust cluster. The system relaxes to the equilibrium in several next ion plasma periods. Note that the total energy is given in arbitrary units (arb. units) normalized to the minimum value of the most stable configuration. This is because the unrealistic ratio of ion to electron mass ~ 200 , nine times lower than the real proton-electron mass ratio, was substituted in PIC simulations affecting the kinetic energy of ions. The computation time is intractably large if a realistic mass ratio is used. A large body of work shows that ratio ~ 120 allows for simulating a realistic process giving credible results [17,18,25,26]. This behavior of the total energy is also observed for the dust clusters consisting of seven, three, and two grains. It is found that the energy minimum is shifted to smaller intergrain separations with decrease of the number of grains in a dust cluster. The cluster consisting of seven grains was most stable with the intergrain separation $\sim 233 \mu\text{m}$. For the dust cluster with three grains, the total energy reaches a minimum at intergrain separations $\sim 2.5\lambda_{D_i}$.

The time evolution of the number of ions and electrons within the computational domain and their kinetic energy are shown in Fig. 5 for energetically favorable configurations of dust clusters with different number of grains. Initially there are $\sim 10^6$ ions and $\sim 10^6$ electrons. During the first several ion plasma periods (~ 20) the number of plasma particles undergoes large fluctuations, reaching then the stationary state. For the dust cluster with three grains, the number of electrons remains $\sim 10^6$, but the number of ions increases by $\sim 2 \times 10^4$. With adding more grains to the cluster, the tendency is that the number of electrons within the computational domain decreases, and the number of ions continues to increase. The dust cluster containing 19 grains equilibrates with isotropic plasma composed of $\sim 1.06 \times 10^6$ ions and $\sim 0.98 \times 10^6$ electrons [Fig. 5(a)]. It should be noted that these deviations in the number of plasma particles occur within the dust

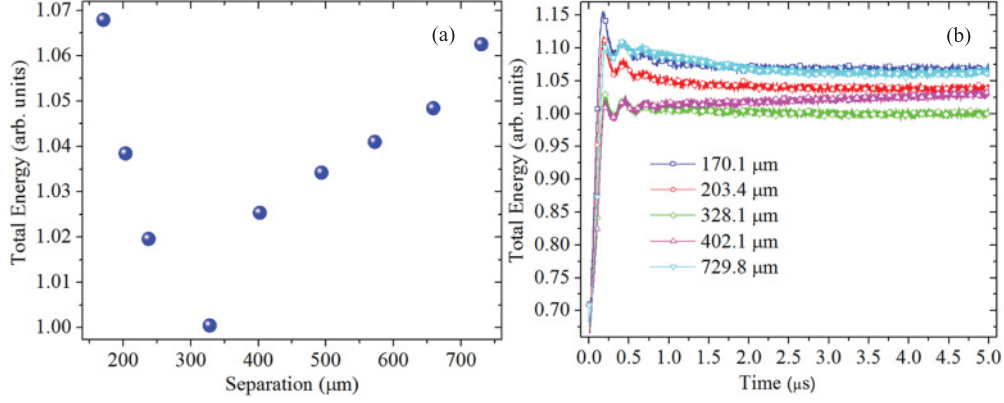


FIG. 4. (Color online) (a) The total energy of the dust-plasma system as a function of the separation distance between 19 grains, and (b) the time evolution of the total energy for different separations in the cluster.

cluster. Thus, the dust cluster of 19 grains immersed in isotropic plasma can be found in the self-confinement state with extra $\sim 6 \times 10^4$ ions and reduced $\sim 2 \times 10^4$ electrons. The absolute value of the charge on grains and the floating potential are reduced by about half compared to the state with well-isolated grains. Under these plasma conditions, the electrostatic repulsion between grains is balanced by their plasma-mediated attraction. In the stationary state, the kinetic energy of ions increases with increasing the number of grains in a dust cluster [Fig. 5(b)]. The contribution comes from the energetic ions moving in the vicinity and within the dust cluster with significantly higher velocities compared to those of thermal ions in the bulk plasma. The kinetic energy of electrons is nearly the same for various clusters [Fig. 5(b)].

IV. DISCUSSION

The Vlasov equation describing the dynamics of plasma in the presence of a finite 2D dust cluster with different intergrain separations was solved using the self-consistent, fully kinetic PIC method. The distribution of plasma ions and electrons in the $\mathbf{x}\text{-}\mathbf{v}$ phase space is followed with time, reaching the steady state. Since the plasma supply from boundaries is continuous, the well-defined steady state is usually reached after $\sim 2 \mu\text{s}$ [Fig. 4(b)]. The total (potential + kinetic) energy of the plasma-grain system is investigated as a function of intergrain separation that we scaled symmetrically around λ_{D_e} . A minimum of the total energy of dust cluster is seen in Fig. 4(a). We started with a cluster configuration in which all the dust grains are well separated ($\sim 2\lambda_{D_e}$). One can expect that the total energy increases constantly for cluster configurations with shorter distances between dust grains. The grains should repel each other at shorter separations due to a large negative charge on them, and there could not be cluster configurations that are energetically favorable. However, to our surprise we discovered that the steady-state total energy of the plasma-grain system [Fig. 4(b)] decreases at shorter separations, reaches a minimum for some configuration of a finite 2D cluster, and then again increases at very short intergrain distances [Fig. 4(a)]. Thus, the energetically favorable state is found with certain intergrain separation, kinetics of plasma ions and electrons within and around a dust cluster, and charge and potential on grains. This is the state with nearly uniform

distribution of ions within a dust cluster as seen in Fig. 2(b). The intergrain separation in the dust cluster was only varied, and the plasma composition adjusts accordingly as well as

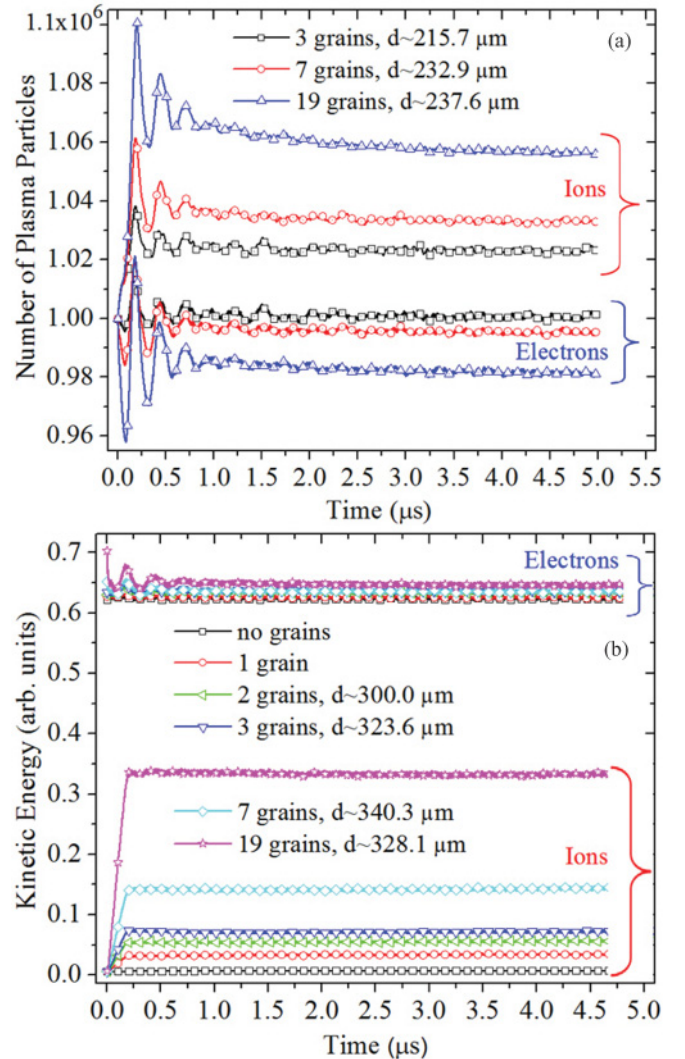


FIG. 5. (Color online) The time evolution of (a) the number and (b) the kinetic energy of ions and electrons in the computational domain with dust clusters containing different number of grains.

the charge and floating potential on grains. The potential distribution within and around a dust cluster was determined by solving the Poisson equation with this peculiar plasma composition and space charge distribution. Analyzing these results, we propose that the energetically favorable configurations are due to the development of a self-consistent state in which the plasma composition and space charge distribution within and around a dust cluster define the distribution of potential and electric field, which, in turn, act as the electric force retaining such plasma composition and charge distribution. In the energetically favorable state, the kinetic effects of plasma ions and electrons overcome the repulsion of grains. The strong grain's repulsion is compensated by the reduced charge and floating potential on grains, overlapped ion clouds screening grains, and depleted electrons within a cluster.

The formation of self-confined dust structures in isotropic plasmas is possible due to the appearance of the common potential boundary confining a dust cluster (Fig. 3). At small separations between grains [Fig. 2(a)], the deep potential well cannot accommodate a sufficient number of ions for suppressing the grain's repulsion. At large intergrain separations, the plasma mediation of grain attractions is insignificant since grains are nearly isolated [Fig. 2(d)]. The energetically favorable configuration develops corresponding to the minimum in total energy (Fig. 4) when the electrostatic repulsion between grains is screened by a uniform cloud of ions localized within the dust cluster [Fig. 2(b)]. We propose that the attraction between dust grains and ion clouds is stronger compared to the grain-grain repulsion. The dust cluster is self-confined in this state on the simulated ion time scale of $\sim 5 \mu\text{s}$. The motion of grains during $\sim 5 \mu\text{s}$ is negligible. Dust grains have a mass which is at least 10 orders of magnitude larger than that of ions. This results in an essential decoupling of the motion of dust grains compared to that of the plasma particles. The plasma can be treated as instantaneously following the motion of heavy dust grains [27]. It was proved theoretically that two "dressed" grains can attract each other when the intergrain separation is $> 2.73\lambda_D$ [7,8], thus strongly supporting our PIC results. In the PIC simulations, we observed such dust grains that are dressed by ion clouds and the energy curve of the plasma-grain system as a function of intergrain separation demonstrates repulsion, minimum, and attraction portions [Fig. 4(a)].

When the separation distance between grains is much smaller than λ_{De} , the plasma composition between grains is completely different compared to that in the bulk plasma. This region is mostly populated by ions and highly depleted of electrons [Fig. 5(a)]. The dust cluster can be considered as a single object with a common plasma sheath formed around grains. The common potential well develops. The potential between closely spaced grains is close to that near the grain's surface. The independent PIC simulation of two dust grains aligned perpendicular to the ion flow with separation $\sim 0.8\lambda_{De}$ [28] indeed shows a common potential well with a very small potential barrier between grains (their Fig. 2, middle). This common potential well is slightly deformed by the directed ion flow, and we presume that it is symmetric in the absence of such ion flow. As the separation increases, the plasma composition between grains transforms gradually to that in the bulk plasma. The strong potential minima and

maxima between grains are clearly seen for large intergrain separations ($\geq 402.1 \mu\text{m}$, Fig. 3).

Our PIC simulations were started with no charge on grains. The buildup of charge, plasma sheath, potential wells on grains, and potential barriers between grains develop during the simulation time. The ion trajectories could be crucially affected on this initial stage of simulation because of the large fluctuations of charge and potential on grains, and the development of multiple potential wells and barriers within a cluster. The motion of ions in the Yukawa-type potential of a single grain was analyzed in detail [29], demonstrating the trajectories such as hyperbola, parabola, folium of Descartes, and Galileo's spiral. These trajectories can be very complicated within a dense multigrain cluster. When the steady state is reached, the charge on grains, potential wells, and barriers continue to fluctuate. The potential maxima can block the trajectories of a small number of ions [30]. Some ions can be temporally trapped and released during such potential fluctuations. These complex issues require further PIC studies.

Despite the fact that under our plasma conditions, the ion mean free path (mfp) is on the order of the size of dust clusters, $\sim 1-2 \text{ mm}$, much longer compared to λ_{De} , the ions are localized in the common potential well. Our PIC model does not include the charge-exchange collisions. The charge-exchange collisions with small but nonzero frequency [30,31] can lead to the trapped ions increasing the ion density near grains by several times. The distribution of ions near a grain with the account for charge-exchange collisions was reported in the PIC simulations and compared to that calculated using the Debye approximation [32]. It was observed that the PIC ion distribution approaches the Debye ion distribution with reduction in the ion mfp. For infinite ion mfp, the collisionless PIC density is about six times smaller compared to that calculated using the Debye distribution [32]. For mfp $\sim 1 \text{ mm}$, the difference reduces to 1.5 times. For mfp $\sim 0.1 \text{ mm}$, the profiles of PIC and Debye ion densities coincide. Thus, the denser ion clouds should be expected near grains with account for charge-exchange collisions and trapped ions. This can enhance the grain screening, reduce the electrostatic repulsion between grains, and strengthen the self-confinement of grains.

V. CONCLUSIONS

We have performed a series of self-consistent, fully kinetic PIC simulations of the plasma-grain and intergrain interactions in dust clusters immersed in isotropic plasmas. No phenomenological adjustable parameters or *ad hoc* assumptions regarding the grain charging, screening, or the form of the interaction potential between grains are used in the PIC model. Our results demonstrate that grains can be trapped in a self-confined state when their ionic clouds overlap forming a uniform cloud of ions within the entire area of a dust cluster. The basic principle of the proposed mechanism responsible for the formation of finite 2D grain clusters is identified as the attraction between grains mediated via their interaction with the surrounding plasma ions. The self-confinement occurs when the common potential well is formed trapping the dust cluster. This point of view is different from an argument that formation of boundary-free dust clusters is due to noncollective attraction (shadow forces) [9,10]. To the best

of our knowledge, a self-consistent fully kinetic PIC modeling of 2D dust clusters was not carried out before. The results reported in the literature are only available for one or two grains or a short chain of grains in a plasma sheath. We believe that our PIC results will inspire other researchers to investigate the self-confinement of dust grains in the isotropic plasma.

The observed self-confined states do not ensure the long-term thermodynamic stability of dust clusters. We need to consider that finite dust clusters are dynamically evolving systems due to the complicated interplay between the charging and screening as well as availability of external sources of plasma particles. It is expected that the self-confinement effect

is of much lower magnitude compared to the confinement by an external potential. Further model simplifications such as the implicit treatment of the plasma can be used to predict the effects of grain motion on the thermodynamic stability of a dust cluster.

ACKNOWLEDGMENTS

This work is supported by the US Department of Energy, Office of Fusion Energy Sciences. TeraGrid computational resources provided by the NCSA under Grant No. TG-PHY090096 are acknowledged.

-
- [1] S. V. Vladimirov and A. A. Samarian, *Plasma Phys. Controlled Fusion* **49**, B95 (2007).
- [2] F. Baletto and R. Ferrando, *Rev. Mod. Phys.* **77**, 371 (2005).
- [3] W.-T. Juan, Z.-H. Huang, J.-W. Hsu, Y.-J. Lai, and I. Lin, *Phys. Rev. E* **58**, R6947 (1998).
- [4] M. Klindworth, A. Melzer, A. Piel, and V. A. Schweigert, *Phys. Rev. B* **61**, 8404 (2000).
- [5] A. Melzer, M. Klindworth, and A. Piel, *Phys. Rev. Lett.* **87**, 115002 (2001).
- [6] V. N. Tsytovich, Ya. K. Khodataev, and R. Bingham, *Comments Plasma Phys. Controlled Fusion* **17**, 249 (1996).
- [7] D. P. Resendes, J. T. Mendonga, and P. K. Shukla, *Phys. Lett. A* **239**, 181 (1998).
- [8] A. S. Ivanov, *Phys. Lett. A* **290**, 304 (2001).
- [9] Ya. K. Khodataev, R. Bingham, V. Tarakanov, V. Tsytovich, and G. Morfill, *Phys. Scr.*, **T 89**, 95 (2001).
- [10] V. N. Tsytovich, N. G. Gousein-zade, and G. E. Morfill, *Phys. Plasmas* **13**, 033503 (2006).
- [11] A. D. Usachev, A. V. Zobnin, V. E. Fortov, O. F. Petrov, B. M. Annaratone, M. H. Thoma, H. Hofner, M. Kretschmer, M. Fink, and G. E. Morfill, *Phys. Rev. Lett.* **102**, 045001 (2009).
- [12] T. Ott, P. Ludwig, H. Kählert, and M. Bonitz, *Molecular Dynamics Simulation of Strongly Correlated Dusty Plasmas*, Introduction to Complex Plasmas, Chap. 10 (Springer-Verlag, Berlin, 2009).
- [13] V. N. Tsytovich, G. E. Morfill, S. V. Vladimirov, and H. Thomas, *Elementary Physics of Complex Plasmas*, Lecture Notes in Physics, Vol. 731 (Springer, Berlin-Heidelberg, 2008).
- [14] S. A. Maiorov, S. V. Vladimirov, and N. F. Cramer, *Phys. Rev. E* **63**, 017401 (2000).
- [15] S. V. Vladimirov, S. A. Maiorov, and O. Ishihara, *Phys. Plasmas* **10**, 3867 (2003).
- [16] C. K. Birdsall and A. B. Langdon, *Plasma Physics via Computer Simulation* (McGraw-Hill, New York, 1985).
- [17] W. J. Miloch, J. Trulsen, and H. L. Péccseli, *Phys. Rev. E* **77**, 056408 (2008).
- [18] W. J. Miloch, *Plasma Phys. Controlled Fusion* **52**, 124004 (2010).
- [19] R. W. Hockney and J. W. Eastwood, *Computer Simulation Using Particles* (McGraw-Hill, New York, 1981).
- [20] G. Joyce, M. Lampe, and G. Ganguli, in *Particle Simulation of Dusty Plasmas*, Space Plasma Simulations, Vol. 615 (Springer-Verlag, Heidelberg, 2002), p. 125.
- [21] K. Matyash, R. Schneider, R. Ikkurthi, L. Lewerentz, and A. Melzer, *Plasma Phys. Controlled. Fusion* **52**, 124016 (2010).
- [22] P. R. Amestoy, A. Guermouche, J.-Y. L'Excellent, and S. Pralet, *Parallel Comput.* **32**, 136 (2006).
- [23] See Supplemental Material at <http://link.aps.org/supplemental/10.1103/PhysRevE.85.056405> for supplementary movies.
- [24] J. D. E. Stokes, A. A. Samarian, and S. V. Vladimirov, *Phys. Rev. E* **78**, 036402 (2008).
- [25] W. J. Miloch, H. L. Péccseli, and J. Trulsen, *Nonlinear Processes Geophys.* **14**, 575 (2007).
- [26] W. J. Miloch, M. Kroll, and D. Block, *Phys. Plasmas* **17**, 103703 (2010).
- [27] M. Bonitz, C. Henning, and D. Block, *Rep. Prog. Phys.* **73**, 066501 (2010).
- [28] W. J. Miloch, S. V. Vladimirov, H. L. Pecseli, and J. Trulsen, *Phys. Plasmas* **16**, 023703 (2009).
- [29] V. E. Fortov, A. V. Ivlev, S. A. Khrapak, A. G. Khrapak, and G. E. Morfill, *Phys. Rep.* **421**, 1 (2005).
- [30] M. Lampe, R. Goswami, Z. Sternovsky, S. Robertson, V. Gavrishchaka, G. Ganguli, and G. Joyce, *Phys. Plasmas* **10**, 1500 (2003).
- [31] J. Goree, *Phys. Rev. Lett.* **69**, 277 (1992).
- [32] S. A. Maiorov, *Plasma Phys. Rep.* **31**, 690 (2005).